Transition barrier at a first-order phase transition in the canonical and microcanonical ensemble

IOP Conf. Series: Journal of Physics: Conf. Series **921** (2017) 012018 doi:10.1088/1742-6596/921/1/012018

Transition barrier at a first-order phase transition in the canonical and microcanonical ensemble

Wolfhard Janke[1], **Philipp Schierz**[1] **and Johannes Zierenberg**[1,2,3]

[1] Institut für Theoretische Physik, Universität Leipzig, Postfach 100 920, 04009 Leipzig, Germany

[2] Max Planck Institute for Dynamics and Self-Organization, Am Fassberg 17, 37077 Göttingen, Germany

[3] Bernstein Center for Computational Neuroscience, Am Fassberg 17, 37077 Göttingen, Germany

E-mail: wolfhard.janke@itp.uni-leipzig.de

Abstract. We compare the transition barrier that accompanies a first-order phase transition in the canonical and microcanonical ensemble. This is directly encoded in the probability distributions of standard Metropolis Monte Carlo simulations and a proper microcanonical sampling technique. For the example of droplet formation, we find that in both ensembles the transition barrier scales as expected but that the barrier is much smaller in the microcanonical ensemble. In addition its growth with system size is weaker which will enhance this difference for larger systems. We provide an intuitive physical explanation for this observation.

1. Introduction

Many relevant transitions in nature fall into the class of first-order phase transitions, where directly at the transition point two or more phases coexist, separated by highly suppressed transition states. Prime examples of first-order transitions include the gas-liquid transition or the change of magnetic order under variation of an external field.

The formation of a droplet in a supersaturated gas is also a first-order phase transition, where instead of coexistence of two pure phases (e.g., gas and liquid) one observes coexistence between the homogeneous gas phase and a phase with a single droplet in equilibrium with the surrounding vapor. While the basic properties of this nucleation process have been thoroughly discussed [1, 2, 3, 4, 5], many puzzling details remain open. In fact, nucleation rates predicted by simulations and measured in experiments still do not match. Classical nucleation theory connects the rate R of droplet formation with the free-energy barrier ΔF: $R = \kappa e^{-\beta\Delta F}$. The kinetic prefactor κ includes the kinetic details of the nucleation process and the free-energy barrier may be related to the suppression in the probability distribution of a suitable reaction coordinate. Both may be, in principle, computed from Monte Carlo simulations [6, 7]. This notion is commonly adapted from the canonical ensemble and we hence refer to the free-energy barrier $\beta\Delta F$ as a general transition barrier B in the following.

In case of the condensation-evaporation transition both the droplet size and the potential energy are suitable reaction coordinates. We focus here on the potential-energy probability distribution $P(E_p)$ and immediately notice that this strongly depends on the thermodynamic ensemble. If the system is in a heat bath (canonical ensemble) there is an exchange of energy

with the surrounding; if the system is isolated (microcanonical ensemble) then there is no energy flux. Of course, in the latter case the system may transfer kinetic to potential energy and vice versa, which allows for a well-defined potential-energy probability distribution.

In the following, we will discuss the effect of the ensemble on the transition barrier of a general first-order phase transition for which the energy is a suitable reaction coordinate. In Sec. 2 we describe a proper microcanonical sampling technique that allows us to obtain the potential-energy probability distribution in both ensembles. Combined with multi-histogram reweighting techniques, we get direct access to the suppression of transition states – the transition barrier. The finite-size scaling is discussed in Sec. 3 followed by an intuitive explanation of the somewhat surprising results. We finish with our conclusions in Sec. 4.

2. Method

We employ Monte Carlo simulations in the "real" microcanonical ensemble [8, 9, 10, 11, 12], referring to the conservation of total energy E which is the standard textbook definition of the microcanonical ensemble. We emphasize this since most previous applications of the microcanonical ensemble in Monte Carlo simulations have focused on the conservation of potential energy E_p. The reason for this will become clear when we briefly discuss the method in the following. In addition to the conservation of the total energy E, we further fix the particle number N and the volume V. This defines the NVE ensemble with the partition function $\Omega(E) = \int\int \mathcal{D}x\ \mathcal{D}p\ \delta(E - [E_p(x) + E_k(p)])$, where $\mathcal{D}x$ denotes the integration over state space and $\mathcal{D}p$ over momentum space. Integrating out the momentum degrees of freedom, which enter the kinetic energy $E_k = \sum_i p_i^2/2m$, this can be reduced to the (restricted) potential-energy space. For N particles in three dimensions one obtains [8]

$$\Omega(E) = \frac{(2\pi m)^{\frac{3N}{2}}}{\Gamma(\frac{3N}{2})} \int_{-\infty}^{\infty} dE_p \hat{\Omega}(E_p)(E - E_p)^{\frac{3N-2}{2}} \Theta(E - E_p), \tag{1}$$

where $\Gamma(n)$ is the Gamma function, $\hat{\Omega}(E_p)$ is the (conformational) density of states and $\Theta(E - E_p)$ is the Heaviside step function reflecting the constraint $E_p \leq E$.

We can thus sample the microcanonical phase space by generating a Markov chain according to the weight

$$W_{\mathrm{NVE}}(E_p) = (E - E_p)^{\frac{3N-2}{2}}\, \Theta(E - E_p), \tag{2}$$

where of course we have to start from a potential energy $E_p < E$ since $E_p > E$ has zero probability in this ensemble. The usual Metropolis acceptance probability for a proposed move from (micro)state A to B is then naturally adapted to the NVE ensemble:

$$P_{\mathrm{acc}}(A \to B) = \min\left\{1, W_{\mathrm{NVE}}(E_p^B)/W_{\mathrm{NVE}}(E_p^A)\right\}. \tag{3}$$

Here one clearly sees the difference to fixing the potential energy in a conformational microcanonical ensemble. While this might be a natural ensemble for spin systems, where a kinetic contribution is not properly defined (but may be exploited for numerical purposes [9]), it is an incomplete ensemble for general systems in soft condensed matter. Of course, a standard Monte Carlo approach in the canonical ensemble makes use of this reduction. This is valid for all canonical expectation values that are independent of the kinetic contributions. However, if one considers quantities that are derived from energy probability distributions, e.g., the free-energy barrier, the contributions of the kinetic energy turn out to play a role [7].

The importance sampling defined in (3) can be combined with a replica-exchange scheme, where parallel simulations at different total energies exchange their configurations with the probability

$$P_{\mathrm{exc}}(A \leftrightarrow B) = \min\left\{1, \frac{W_{\mathrm{NVE^B}}(E_p^A) W_{\mathrm{NVE^A}}(E_p^B)}{W_{\mathrm{NVE^B}}(E_p^B) W_{\mathrm{NVE^A}}(E_p^A)}\right\}. \tag{4}$$

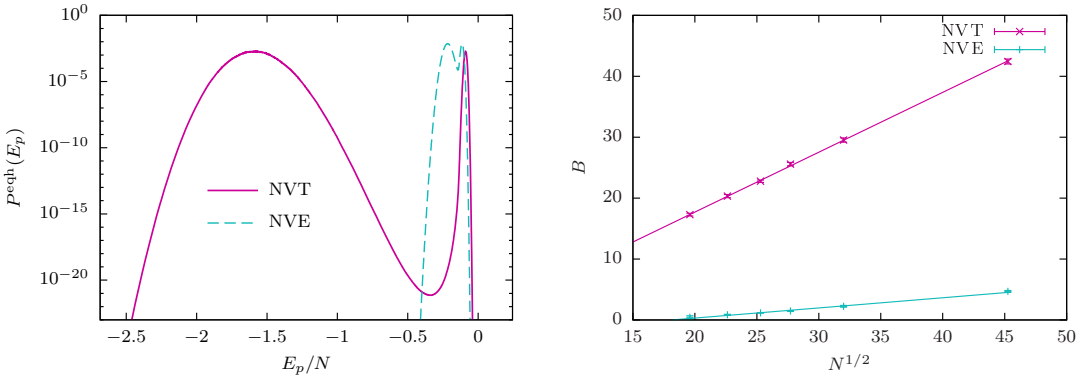

Figure 1. (left) Probability distributions of the potential energy in the canonical (NVT) and microcanonical (NVE) ensemble for 2048 Lennard-Jones particles at fixed density $\rho = 10^{-2}$. The distributions are obtained at the equal-height temperature $T_{\mathrm{eqh}} = 0.6175$ and equal-height total energy $E_{\mathrm{eqh}}/N = 0.6849$, respectively. (right) The free-energy barrier of the condensation-evaporation transition in a Lennard-Jones system for the (conformational) NVT and NVE ensembles. This is directly related to the sampling barrier in the respective importance sampling schemes.

Afterwards, NVE WHAM can be applied to estimate the density of states $\hat{\Omega}(E_p)$ [10, 13, 14, 15]. This is an ensemble-independent property of the simulated system and allows one to estimate observables in other ensembles, e.g., the canonical NVT ensemble [10, 16].

3. Results

As an illustrative example we show results for the 12–6 Lennard-Jones particle system where the particles i and j interact via the potential $V_{\mathrm{LJ}}(r_{ij}) = 4\epsilon\left[(\sigma/r_{ij})^{12} - (\sigma/r_{ij})^{6}\right]$, cutoff and shifted at $r_{ij} = 2.5\sigma$, with $\epsilon = 1$ setting the energy (or temperature) and $\sigma = 2^{-1/6}$ setting the length scale of the system. We consider N particles in a cubic box of volume V with periodic boundary conditions and fix the density to $\rho = N/V = 0.01$. To update the particle positions, we apply short-range displacement and long-range jump proposals, with symmetric selection probabilities each. The combination of replica-exchange NVE sampling and NVE WHAM allows us to directly estimate the potential-energy probability distribution in both the canonical ensemble, $P_{\mathrm{NVT}}(E_p) \propto \hat{\Omega}(E_p)\exp(-E_p/k_BT)$, and microcanonical ensemble, $P_{\mathrm{NVE}}(E_p) \propto \hat{\Omega}(E_p)W_{\mathrm{NVE}}(E_p)$. Both show, as expected, a double peak at the condensation-evaporation transition, see Fig. 1 (left). In the canonical ensemble, we have to vary the temperature to obtain a wide distribution with pronounced peaks of equal height at $T_{\mathrm{eqh}} = 0.6175$. In the microcanonical ensemble, we vary the total energy to obtain a comparably narrow double-peak distribution at $E_{\mathrm{eqh}}/N = 0.6849$.

In addition to being much narrower, we also notice that the suppression of transition states in the microcanonical probability distribution is much lower than in the canonical distribution. This corresponds to a much lower barrier $B_{\mathrm{NVE}} \ll B_{\mathrm{NVT}}$, each defined by

$$B = \ln\left[P^{\mathrm{eqh}}\left(E_p^{\pm}\right)/P^{\mathrm{eqh}}\left(E_p^{0}\right)\right], \tag{5}$$

where $P^{\mathrm{eqh}}(E_p)$ is the (equal-height) potential-energy distribution in the respective ensemble, $E_p^{\pm}$ refers to the location of the two maxima and E_p^0 to the location of the minimum in between. Figure 1 (right) shows the canonical and microcanonical barriers for system sizes $N \in \{384, 512, 640, 768, 1024, 2048\}$. The microcanonical barrier is always below the canonical

barrier. In fact, the suppression is several orders of magnitude smaller as best illustrated for the $N = 2048$ system where $B_{\mathrm{NVT}} = 42.4$ and $B_{\mathrm{NVE}} = 4.7$ – recall that this measures the logarithm of the suppression. In this case, importance sampling in the NVE ensemble is of the order of 10^{16} times more efficient than in the canonical counterpart for this transition. This observation can be derived from the ensemble weights [11] and thus is generally true for any first-order phase transition with suppressed transition states in the energy probability distribution. It can be further generalized to any properly defined probability distribution and tailored ensemble weight.

From the canonical ensemble we know that the barrier is related to the surface of the interface that separates the coexisting phases, here the liquid droplet from the surrounding gas. We expect that the barrier is thus proportional to the surface of the droplet, $B \propto \partial V_D$. The surface depends on the droplet volume, $\partial V_D \propto V_D^{2/3}$. Due to the interplay of energy minimization inside the droplet and entropy maximization in the surrounding gas, the droplet volume is expected to grow with system size as $V_D \propto V^{3/4}$ [17, 18, 19, 20], or at fixed density as $V_D \propto N^{3/4}$ [21]. Introducing an effective interfacial free energy τ and considering additional logarithmic corrections [22, 23, 24, 25, 26] we arrive at the finite-size scaling ansatz in the canonical ensemble [7]

$$B = \tau N^{1/2} - \alpha \ln N + c, \tag{6}$$

where α and c are constants.

In the microcanonical ensemble, the setup directly at the transition energy is very similar to the canonical ensemble: A fixed volume and particle number, while the system switches between a homogeneous gas and a droplet in coexistence with the surrounding vapor. In fact, the conservation of total energy introduces a potential-energy reservoir from which the system can take potential energy to form a droplet or where it can store it to form a gas. In a limited scope, this is locally comparable to the canonical ensemble. We hence assume the same dependence of the barrier on the droplet surface, which trivially scales with the droplet volume. The relation between droplet size and system size is as well assumed to be consistent with the canonical ensemble, assuming the energy and entropy arguments to be transferable. We thus assume the same scaling ansatz (6).

Figure 1 (right) shows the canonical and microcanonical barriers which satisfy to leading order the scaling ansatz (6). For simplicity, we only consider a few system sizes and restrict fits to the effective behavior $B = \tau N^{1/2} + c$, which yields $\tau_{\mathrm{NVT}} = 0.98(2)$ and $\tau_{\mathrm{NVE}} = 0.166(8)$, with goodness-of-fit parameters $Q \approx 0.79$ and $Q \approx 0.18$, respectively. Please note that we here focus on the conformational canonical ensemble because of the direct relation to the Monte Carlo sampling methods. Working with the full canonical ensemble, however, only shifts the line but leaves the τ estimate invariant [7].

Let us finally give a physical picture that heuristically explains the difference of the sampling behavior in the NVT and NVE ensembles for the droplet condensation-evaporation transition. In the NVT ensemble, the system is in a heat bath, which ensures that there is always energy available to be added to the system. The result is a constant transition probability to higher potential-energy configurations with the same energy step ΔE_p independent of the specific value of the potential energy. At the canonical transition temperature, this allows in principle to transform the coexisting (possibly large) droplet at low potential energy into a gas with high potential energy. The situation is different in the NVE ensemble, where a distinct amount of energy is available and distributed in potential and kinetic energy. The potential energy may only be raised by transferring kinetic energy with decreasing probability until none is left. This puts an upper bound on the reachable potential energies. The result is a decreasing transition probability to higher potential-energy configurations which therefore depends on the current potential energy and goes to zero when approaching the upper bound. At the point where the energy versus entropy competition evens out in the NVT ensemble, the NVE ensemble will still

be stuck in the droplet phase since higher energies show a higher suppression. Consequently, phase coexistence occurs in the NVE ensemble at a smaller droplet size, which explains the smaller barrier.

4. Conclusions

We demonstrated on the example of the condensation-evaporation transition that the transition barrier of a first-order phase transition is always smaller in the microcanonical ensemble compared to the canonical ensemble. In fact, a finite-size scaling analysis reveals that this effect drastically increases in the limit of increasing system sizes. A physical reason for this is that in a heat bath (canonical ensemble) the system can in principle increase its potential energy infinitely, because there is an infinite reservoir of potential energy – the heat bath. In the microcanonical ensemble, the finite reservoir of potential energy due to the constraint of a fixed total energy allows only very narrow distributions with a reduced barrier [11]. These general statements about the ensembles are not restricted to computational considerations. Physical microcanonical signatures might be approximately observed in astrophysics or extremely isolated systems on earth where the barrier difference should show up as well.

Acknowledgments

This work has been partially supported by the DFG (Grant No. JA 483/31-1), the Leipzig Graduate School "BuildMoNa", and the Deutsch-Französische Hochschule DFH-UFA (Grant No. CDFA-02-07). The authors gratefully acknowledge the computing time provided by the John von Neumann Institute for Computing (NIC) on the supercomputer JURECA at Jülich Supercomputing Centre (JSC) under Grant No. HLZ24. JZ received financial support from the German Ministry of Education and Research (BMBF) via the Bernstein Center for Computational Neuroscience (BCCN) Göttingen under Grant No. 01GQ1005B.

References

[1] Volmer M and Weber A 1925 *Z. Phys. Chem.* **119** 277
[2] Becker R and Döring W 1935 *Ann. Phys.* **416** 719
[3] Feder J, Russell K C, Lothe J and Pound G M 1966 *Adv. Phys.* **15** 111
[4] Oxtoby D W 1992 *J. Phys: Condens. Matter* **4** 7627
[5] Kashchiev D 2000 *Nucleation: Basic Theory with Applications* (Oxford: Butterworth-Heinemann)
[6] Auer F and Frenkel D 2001 *Nature* **409** 1020
[7] Zierenberg J, Schierz P and Janke W 2017 *Nat. Commun.* **8** 14546
[8] Calvo F, Neirotti J P, Freeman D L and Doll J D 2000 *J. Chem. Phys.* **112** 10350
[9] Martin-Mayor V 2007 *Phys. Rev. Lett.* **98** 137207
[10] Schierz P, Zierenberg J and Janke W 2015 *J. Chem. Phys.* **143** 134114
[11] Schierz P, Zierenberg J and Janke W 2016 *Phys. Rev.* E **94** 021301(R)
[12] Davis S and Gutiérrez G 2017 *arXiv*:1703.05992
[13] Ferrenberg A M and Swendsen R H 1989 *Phys. Rev. Lett.* **63** 1195
[14] Kumar S, Rosenberg J M, Bouzida D, Swendsen R H and Kollman P A 1992 *J. Comput. Chem.* **13** 1011
[15] Kim J, Straub J E and Keyes T 2012 *J. Phys. Chem.* B **116** 8646
[16] Escobedo F A 2006 *Phys. Rev.* E **73** 056701
[17] Biskup M, Chayes L and Kotecký R 2002 *Europhys. Lett.* **60** 21
[18] Biskup M, Chayes L and Kotecký R 2003 *Commun. Math. Phys.* **242** 137
[19] Neuhaus T and Hager J S 2003 *J. Stat. Phys.* **113** 47
[20] Binder K 2003 *Physica* A **319** 99
[21] Zierenberg J and Janke W 2015 *Phys. Rev.* E **92** 012134
[22] Langer J S 1967 *Ann. Phys. N.Y.* **41** 108
[23] Ryu S and Cai W 2010 *Phys. Rev.* E **81** 030601(R)
[24] Nußbaumer A, Bittner E and Janke W 2010 *Prog. Theor. Phys. Suppl.* **184** 400
[25] Prestipino S, Laio A and Tosatti E 2012 *Phys. Rev. Lett.* **108** 225701
[26] Prestipino S, Laio A and Tosatti E 2014 *J. Chem. Phys.* **140** 094501